International Journal of Basic and Applied Chemical Sciences ISSN: 2277-2073 (Online)
An Open Access, Online International Journal Available at http://www.cibtech.org/jcs.htm
2017 Vol. 7(4) October-December, pp.1-13/Liu and Pang
Research Article

THE INFLUENCE AND INTERACTION BETWEEN FERRIC NITRATE MODIFIED EXPANDABLE GRAPHITE AND AMMONIUM POLYPHOSPHATE ON FLAME RETARDANCY AND THERMAL STABILITY OF LLDPE

Jianing Liu[1,2] and *Xiuyan Pang[1]
[1]Department of Chemistry and Environmental Science, Hebei University, Baoding 071002, China
[2]Lucky Film Co. Ltd, Baoding, Hebei 071054, China
**Author for Correspondence*

ABSTRACT
Ferric nitrate modified expendable graphite (EG_{Fe}) was prepared through the oxidation and intercalation of natural graphite, and its dilatability, crystal structure, main intercalated elements and functional groups were represented respectively. Its influence and synergistic effect with ammonium polyphosphate (APP) on the combustion behavior and thermal stability of linear low density polyethylene (LLDPE) were investigated. Results reveal EG_{Fe} show better dilatability, environment-friendly property and flame retardancy than the normal expandable graphite (EG). A 30 wt % EG_{Fe} improves the limiting oxygen index (LOI) of LLDPE from 17.5% to 27.5%. Especially, when used in combination with APP, there is a synergistic effect between these two flame retardants, it improves the LOI of 70LLDPE/15APP/15EG_{Fe} to 30.5% and the vertical combustion UL-94 level to V-0. The thermal gravimetric/differential thermal gravimetric analysis results confirm that EG_{Fe}, mixture of EG_{Fe} and APP are beneficial for the improvement of composite thermal stability. The Fe_2O_3, a decomposing product of $Fe(NO_3)_3$, can impel the APP decomposition reaction and then form stable polyphosphate. The interstitial filling of Fe_2O_3, polyphosphate, together with the conglutination between loose "graphite worms" and polyphosphoric acid generate the continuous and compact char layers, which makes 70LLDPE/15APP/15EG_{Fe} composite show excellent flame retardation.

Keywords: *Modified Expandable Graphite, Ferric Nitrate, Ammonium Polyphosphate, Polyolefin, Synergistic Performance*

INTRODUCTION
Flame retardants (FRs) are added to materials in order to prevent combustion and delay the spread of fire after ignition (Kemmlein *et al.,* 2003). Through the years, intumescent flame retardants (IFRs) have attracted much attention not only because they are environmentally friendly, but also they are more efficient than inorganic FRs (Gao *et al.,* 2011; Liu *et al.,* 2016). On heating, IFR will form a foamed cellular charred layer on the surface of the substrate, which can decelerate heat and mass transfer between the gaseous and condensed phases (Duquesne *et al.,* 2003; Shi *et al.,* 2006). Ammonium polyphosphate (APP) is an effective IFR for polymer materials (Zhang *et al.,* 2013; Lu *et al.,* 2014), and its efficiency is generally attributed to the increase in the char formation through involving in altering the pathway of the thermal degradation of the substrate and promoting solid-state reaction leading to carbonization (Camino *et al.,* 1990; Horacek and Grabner, 1996; Gaan *et al.,* 2008). However, the flame retardation of APP for polyolefin is very limited due to the absence of oxygenous groups in matrix and resulting in the insufficient protective layer (Nie *et al.,* 2008; Zheng *et al.,* 2013).
The graphite intercalation compound (GIC), named expandable graphite (EG), is another kind of IFR with good capability such as halogen-free, non-dropping and low-smoke. When it's used as FR, EG plays multiple roles of char-forming agent, blowing agent and smoke suppressant (Chen *et al.,* 2007; Ge *et al.,* 2012). When contacting a flame source, the EG will instantly expand and release noncombustible H_2O and CO_2 gases to dilute the concentration of the volatile flammable compositions. At the same time, the flake EG particles turn into swollen "worm like" expanded graphite, which causes protection for matrix surface from the covered multicellular char. Due to its outstanding capability, EG has been used in the

flame retardation of various polymer materials (Xie and Qu, 2001; Modesti *et al.*, 2002; Zhang *et al.*, 2013; Sun *et al.*, 2014). Whereas, there are some problems need to be solved. In the preparation of EG, H_2SO_4 is the most commonly used oxider, H^+ donor and intercalation agent due to its low-price, strong oxidizability and well dilatability of the obtained product (Shioyam and Fujii, 1987). However, the use of it normally leads to high sulfur content in EG and corrosion for storage devices. Besides, more SO_2 gas will release in oxidation reaction between H_2SO_4 and graphite atom (Song *et al.*, 1996). Furthermore, the formed multicellular "graphite worms" chars are loose and easy to collapse and even flow away under the influence of flame pressure or heat convection, which leads to the loss of residual char and decreases the efficiency in slowing down heat and mass transfer, and then the fire protection would significantly depress. Therefore, a more than 20 wt % dose is added in order to achieve satisfying effect, which normally leads to obvious deterioration of the mechanical properties owing to the existed "popcorn effect" (Sun *et al.*, 2014; Xu *et al.*, 2013). Therefore, the intercalation reaction requires modification to improve EG efficiency and environmental friendliness at the same time.

The wide intercalation possibilities permit the GIC to possess definite properties (Shornikova *et al.*, 2006). The assistant intercalation of the second non-carbon substance (called assistant intercalator) can normally improve the dilatability and its flame retardation for matrix. It was reported the H_2SO_4/APP (APP, an assistant intercalator) intercalated EG, prepared through two-step method, exhibited a higher expansion volume (EV) of 240 mL/g than that of normal EG (the H_2SO_4 intercalated GIC) of 210 mL/g (Han *et al.*, 2007). Moreover, the H_2SO_4/borate modified EG presented a higher EV of 515 mL/g and LOI of 28.4% for LLDPE than that of the normal H_2SO_4 intercalated EG with an EV of 400 mL/g and LOI of 26.0% (Pang *et al.*, 2015).

At the same time, addition of EG together with APP is an efficient method to improve the flame retardancy (Lu *et al.*, 2014; Hu and Wang, 2013). As mentioned above, the efficiency of single APP for polyolefin is very limited due to the absence of char forming agent and oxygenous groups in matrix (Nie *et al.*, 2008; Lai *et al.*, 2015). Whereas, the combination of EG with APP can remedy this limitation. EG normally possesses a low expansion temperature than APP, the swollen "graphite worms" produced in advance can act as char forming agent. The subsequent polyphosphoric acids coming from APP decomposition reaction will produce conglutination between the loose "graphite worms", enhance the continuous, compact of residue layers, and then improve the flame retardation (Meng *et al.*, 2009; Seefeldt *et al.*, 2012; Tang *et al.*, 2016).

As one of transition metal oxides, Fe_2O_3 has obvious impact on the thermal decomposition process of APP (Ebert, 1976). It can accelerate the release of NH_3 and H_2O in the earlier period, and increase the high temperature residue in the later period due to the formation of metallic phosphate. In view of the improvement of Fe_2O_3 for APP flame retardancy and the influence of assistant intercalator on EG dilatability and flame retarded efficiency, the main purpose of this research was to prepare a ferric nitrate modified GIC (written as EG_{Fe}) through graphite intercalation reaction (Shornikova *et al.*, 2006). Then, investigate its flame retardancy, synergistic effect with APP, and further get the FRs formula corresponding to achieving a satisfied LOI value and UL-94 level.

MATERIALS AND METHODS

Materials and Reagents

Natural flake graphite with average particle size of 0.30 mm and carbon content of 96 wt% was provided by Xite Carbon CO. LTD, Qingdao, China. LLDPE (920NT(EGF-34), melt index 0.2 g/min) was purchased from Sinopec Sabic Tianjin Petrochemical. APP (II, n>1000) was purchased from Sichuan Shifang. $Fe(NO_3)_3{\cdot}9H_2O$, $KMnO_4$ and H_2SO_4 (98 wt %) were all analytical agents and used as received.

Preparation of the EG_{Fe} and EG

Firstly, the reactants were weighed according to a definite mass ratio of graphite (C): H_2SO_4 (98 wt %): $KMnO_4$: $Fe(NO_3)_3{\cdot}9H_2O$, and H_2SO_4 was diluted to a demanded mass concentration with deionized water and cooled to room temperature before use. Then, the quantified reactants were mixed in the order of diluted H_2SO_4, C, $KMnO_4$ and $Fe(NO_3)_3{\cdot}9H_2O$ in beaker and stirred at a certain temperature controlled by

a water bath. When the reaction finished, the solid phase was washed with deionized water and dipped in water for 2.0 h until pH value of the waste water reached to 6.0-7.0, then, filtrated and dried at 50-60 °C for 5.0 h. The influence of various factors on dilatability of the EG_{Fe} were optimized through single-factor tests including the dose of H_2SO_4 (98 wt %), $KMnO_4$, $Fe(NO_3)_3{\cdot}9H_2O$ and H_2SO_4 concentration, reaction temperature and time. Feasible conditions of EG_{Fe} preparation were finally identified as: mass ratio of C: $KMnO_4$: H_2SO_4 (98 wt %): $Fe(NO_3)_3{\cdot}9H_2O$ was 1.0:0.27:5.0:0.17; H_2SO_4 was diluted to 75 wt % before reaction; intercalation reaction was totally maintained for 40 min at 40 °C. Product's initiation expansion temperature and EV at 800 °C are detected as 170 °C and 530 mL/g respectively (Pang *et al.*, 2015).

Compared with EG_{Fe}, the single H_2SO_4 intercalated EG was prepared at the mass ratio C: $KMnO_4$: H_2SO_4 (98 wt %) of 1.0:0.27:5.0 under the same condition as mentioned in the preparation of EG_{Fe}. Its initial expansion temperature and EV were 180 °C and 480 mL/g respectively. Obviously, addition of assistant intercalator has significant influence on dilatability, reflected by the increase of EV and change of initial expansion temperature. It's speculated that EG_{Fe} will form thicker intumesce char than the normal EG, and then show better flame retardancy.

Preparation of the Flame Retarded LLDPE Composites

A certain amount of FRs were added into melted LLDPE at 120 °C in Muller, the mixtures were pressed at 125 °C and 10 MPa, and then chopped into slivers with two different sizes of 120.0×6.0×3.0 mm^3 and 127.0×13.0×3.0 mm^3 for the evaluation of combustion performance.

Measurements and Characterization of Different Properties

Scanning slectron microscope (SEM) TM3000 (Japan) was applied to observe layer structures of natural graphite and EG_{Fe}. Moreover, it was employed to survey the residue micromorphology. A digital camera was employed to survey the residues macromorphology.

The energy dispersive spectroscopy (EDS) of C, N, O, S, Fe, and so on in natural graphite, EG_{Fe} and the EG was detected with JSM-7500F instrument under an accelerating voltage of 20 kV. The detector resolution and the element detection range were 132 eV and from B to U respectively. Prior to observation, sample surfaces were coated with a conductive material.

Fourier transform infrared (FTIR) spectra of the prepared GICs and the residual chars of the flame retarded LLDPE composites after their combustion tests were recorded between 4000-400 cm^{-1} using a FTIR spectrometer (Nicolet 380, America Thermo Electron Corporation) with a resolution of 2 cm^{-1}. Samples were prepared by mixture of the sample powder and KBr at a mass ratio of about 1:100.

X-ray diffraction (XRD) pattern of the prepared GICs was obtained with an Y2000 X-ray diffractometer (Dandong, China) under the operation condition of 40 kV, 30 mA, employing Ni-filtered Cu K_α radiation with 2θ ranging from 20° to 70°. The interlayer spacing was obtained from the angle at which the corresponding peak was diffracted.

LOI test was used to evaluate the combustion property of the flame retarded LLDPE composites with a size of 120.0×6.0×3.0 mm^3, and it was detected using a JF-3 LOI instrument (Chengde, China) according to Standard of GB/T2406-1993. At the same time, vertical combustion UL-94 level tests were performed using a HC-3 vertical burning instrument (Tientsin, China) on sheets of size 127.0×13.0×3.0 mm^3 as per the standard UL 94-1996.

The thermal gravimetric and differential thermal gravimetric (TG/DTG) analysis were carried out with a STA 449C instrument (Germany), about 5.0 mg sample was detected under N_2 atmosphere with a flux of 25 mL/min. It was heated from about 40 °C to 800 °C at a heating rate of 10 °C/min. Changes of sample weight as temperature were recorded.

RESULTS AND DISCUSSION

Characterizations of Natural Graphite and Its GICs

*Crystal Structure***:** Figure 1 presents the cross-section electron microscope photographs of natural graphite with a magnification of 20000 times in Figure 1 (a) and EG_{Fe} with a magnification of 2000 times in Figure 1 (b). The layer structures of natural graphite are compact and the layer distance is very small and regular. It can be speculated that there is strong force between the carbon layers. The layer distance of

EG_{Fe}, by contrast, has been enlarged, and boundary layers are loose and seriously damaged, which should be caused by the oxidation and intercalation reaction. Therefore, the force between the carbon layers is relatively weaker than that of the natural graphite. Moreover, when heated, it will show dilatability.

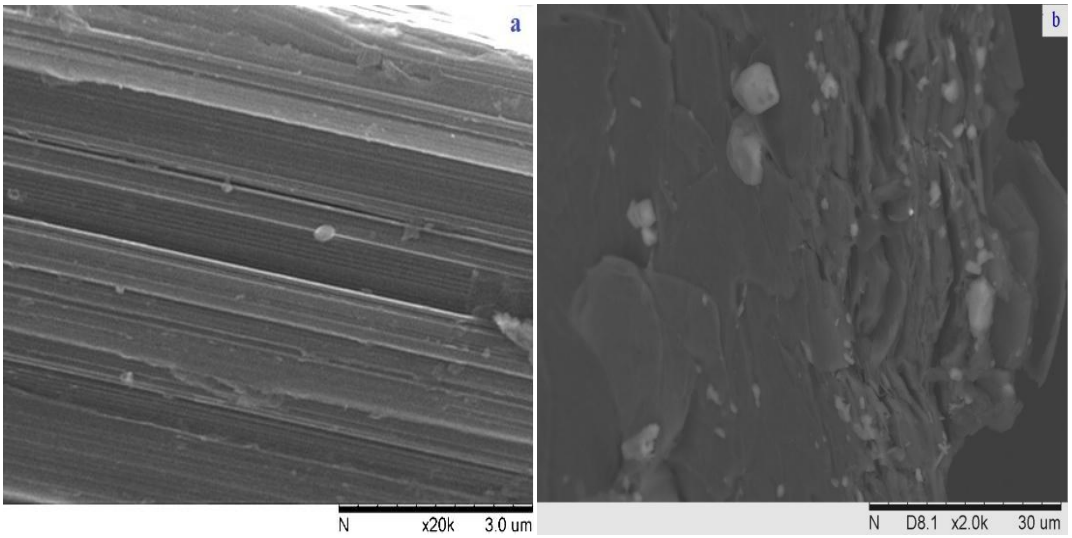

Figure 1: SEM Photographs of Natural Graphite (a) and the EG_{Fe} (b)

EDS Analysis: EDS results listed in Table 1 present the main surface elements and their relative percentage composition in natural graphite, the prepared EG and EG_{Fe} respectively. As can be seen in Table 1, besides C element, natural graphite still consists of a little of S, O, Mn, Si and Ca. In the EG, contents of O and S are relative higher than that of natural graphite, which reveals the intercalation of H_2SO_4/HSO_4^- (Shioyam and Fujii, 1987). As for the EG_{Fe}, contents of S and O are also higher, especially for O. Moreover, Fe element are detected in EG_{Fe}, and its S content is lower than that of EG due to the assistant intercalation of $Fe(NO_3)_3$. The N element is not detected in all the three samples for its poor content and weak sensitivity.

Table 1: Surface Composition of Natural Graphite and the Prepared GICs[a]

Elements	**Samples**		
/%	**Natural Graphite**	**EG**	**EG_{Fe}**
C	96.3	88.97	87.94
O	0.60	8.97	9.69
S	0.42	1.79	1.50
Ca	0.72	N.D.	N.D.
Si	0.38	N.D.	N.D.
Fe	N.D.	N.D.	0.57
N	N.D.	N.D.	N.D.
Mn	1.58	0.27	0.30
Total	100	100	100

[a]N.D.: not detected.

FTIR Analysis: Figure 2 shows FTIR spectra of the prepared EG and EG_{Fe}. The two samples both show the characteristic stretching vibrations absorption peaks of -OH (about 3430 cm^{-1}) and S=O (about 1143 cm^{-1}) caused by intercalation of H_2SO_4/HSO_4^- (Shioyam and Fujii, 1987; Ebert, 1976). At the same time, the peaks at about 1620 cm^{-1} are the specific absorption of C=C stretching vibrations, and it has shifted to a smaller wave number due to the graphite conjugated structure. It's worth noting that the characteristic

stretching vibration absorption of NO_3^- is observed at 829 cm^{-1}, and specific absorption of the Fe-O appears at 721 cm^{-1} and 559 cm^{-1} as well (Willeams and Fleing, 2001). These results confirm the intercalation of the intercalator and the assistant intercalator.

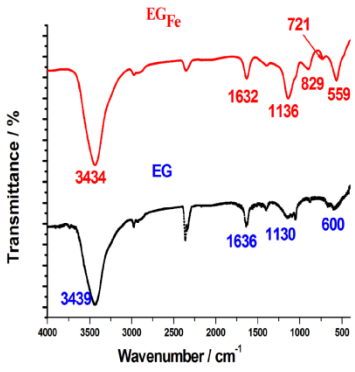

Figure 2: FTIR Analysis of the Prepared EG and EG_{Fe}

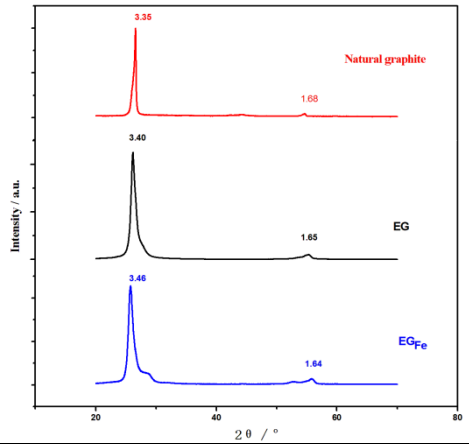

Figure 3: XRD Analysis of Natural Graphite, the EG and EG_{Fe}

XRD Analysis: As showed in Figure 3, EG_{Fe} and the referenced EG show the same characteristic diffraction peaks like natural graphite at about 26.6º and 55º, which indicates that they all keep the layer structures. Whereas, it is worthy to note that the (002) diffraction peaks transfer to small angles of 26.2° for the EG and 25.8° for EG_{Fe} respectively. At the same time, each corresponds to a big interplanar spacing of 3.40 Å for EG and 3.46 Å for EG_{Fe}. The XRD results confirm that intercalators have been inserted into graphite layers, and the EG_{Fe} possesses bigger interplanar spacing for the assistant intercalation of $Fe(NO_3)_3$.

Combustion Behavior

The influence of EG_{Fe} and other FRs on combustion behavior of LLDPE was evaluated in LOI and vertical combustion UL-94 tests, and the results were showed in Table 2. LLDPE is very flammable with a LOI of 17.5%, and additionally, the combustion accompanies with serious melt-dropping as showed in Figure 4 (a). While, addition of the tested FRs can all affect combustion process. Addition of the referenced EG at 30 wt % leads LOI value of the 70LLDPE/30EG composite to 25.5%, and the melt-dropping, ignition is basically under control. Addition of the same amount of EG_{Fe} can not only improve the UL-94 level to V-2, but also increase the LOI value to 27.5%. These results indicate the assistant intercalation of $Fe(NO_3)_3$ ameliorates the flame retardation of EG_{Fe}. Addition of the prepared GICs can all reduce the melt-dropping phenomena, which should be attributed to the protective intumescent carbonaceous char formed on polymer surface by EG or EG_{Fe} expansion as showed in Figure 4 (c) and Figure 4 (d).

It can be seen that independent APP presents a weak efficiency for LLDPE. When it's solely added at 30 wt %, LOI value of the 70LLDPE/30APP specimen is only 20%, and accompanied by melt-dropping and ignition as showed in Figure 4 (b). The limited efficiency for LLDPE is due to the absence of protection char layer. While, additions of EG_{Fe} and APP at different wt % can not only increase LOI value, but also improve all specimens UL-94 level to V-0 simultaneously. Noticeably, these LOI values are obviously higher than the theoritical calculated LOI_{the}, calculated according to FR wt % and LOI values of 70LLDPE/30APP and 70LLDPE/30EG_{Fe} (Menachem, 2001). Therefore, it can be inferred that there is synergistic efficiency between these two FRs. Meanwhile, the APP and EG_{Fe} ratio has an important influence on flame retardancy, and the tested optimum mass ratio is 15:15 as showed in 70LLDPE/15APP/15EG_{Fe} specimen, the LOI value and UL-94 level can reach 30.5% and V-0 respectively.

Table 2: Specimens Combustion Characteristics[b]

Specimens	LOI %		UL-94 level
	LOI_{exp}	LOI_{the}	
100LLDPE	17.5	N.D.	N.D.
70LLDPE/30APP	20	N.D.	N.D.
70LLDPE/30EG	25.5	N.D.	V-2
70LLDPE/30EG_{Fe}	27.5	N.D.	V-2
70LLDPE/10APP/20EG_{Fe}	29	25.0	V-0
70LLDPE/15APP/15EG_{Fe}	30.5	23.8	V-0
70LLDPE/20APP/10EG_{Fe}	28.5	22.5	V-0

[b] LOI_{exp}: the LOI value detected in test.

LOI_{the}: the LOI value calculated.

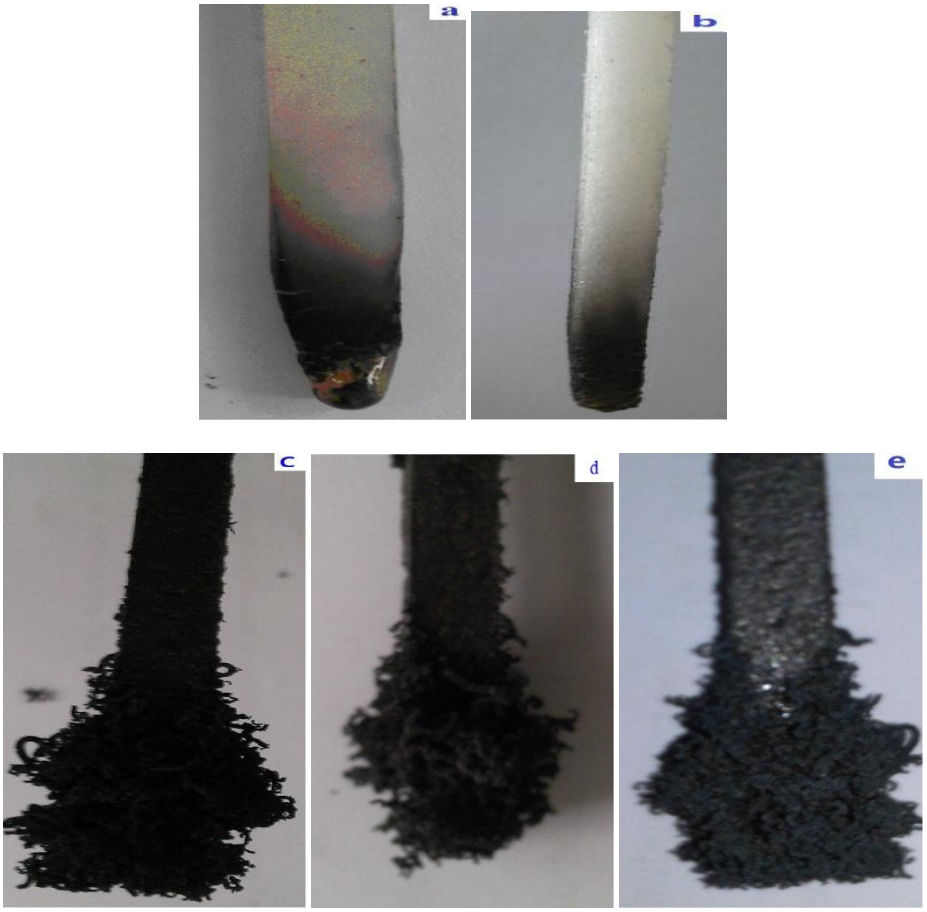

Figure 4: The Macromorphology of LLDPE Specimens in Vertical Combustion Tests LLDPE (a), 70LLDPE/30APP (b), 70LLDPE/30EG (c), 70LLDPE/30EG_{Fe} (d), 70LLDPE/15APP/15EG_{Fe} (e)

Combustion Residue Micromorphology

In combustion process, the char morphology has important influence on flame retardation. Therefore, residual incision micromorphology of 70LLDPE/30EG, 70LLDPE/30EG_{Fe} and 70LLDPE/15APP/15EG_{Fe} after their combustion tests are recorded by SEM. As showed in Figure 5 (a) and 5 (b), a regular and discontinuous "open-cellular" structure showing the "popcorn effect" on the surface is observed in 70LLDPE/30EG and 70LLDPE/30EG_{Fe} due to the expansion of EG and EG_{Fe}. The discontinuous residues

can cause the decrease of shielding function for heat and mass transfer. Although, the EG_{Fe} can improve the UL 94 level to V-2, there is still melt dropping caused by the collapse and float of the incompact residue. The incision of 70LLDPE/15APP/15EG_{Fe} showed in Figure 5 (c) is relatively continuous and compact due to the conglutination of APP decomposition products; this structure can suppress the mentioned "popcorn effect" to a certain extent, and then provide a better shield that insulates the substrate from radiant heat, further avoid the direct contact between substrate and flame. It is the continuous and compact residual that makes 70LLDPE/15APP/15EG_{Fe} composite hold higher LOI value than the other flame retarded composites.

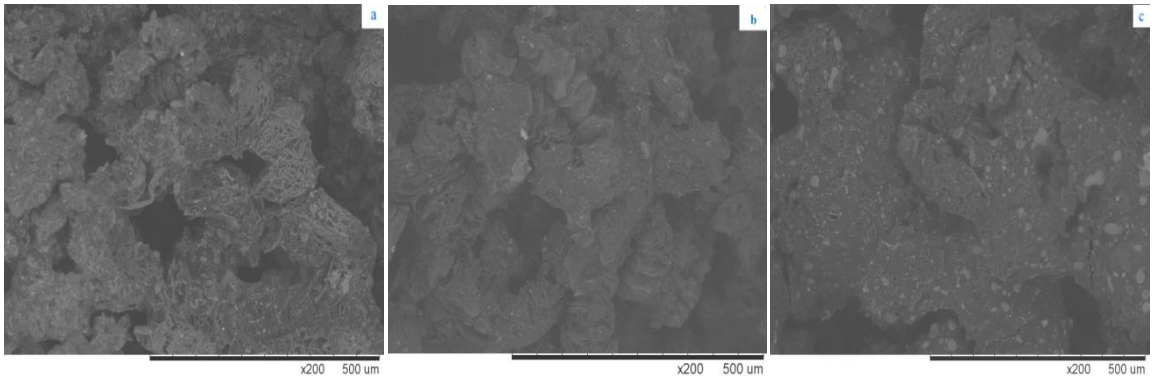

Figure 5: Incision Section Micromorphology of 70LLDPE/30EG (a), 70LLDPE/30EG_{Fe} (b) and 70LLDPE/15APP/15EG_{Fe} (c) after Combustion Tests

FTIR Analysis for Combustion Residues

Further information obtained from FTIR analysis about the chemical composition and functional groups of the combustion residues were showed in Figure 6. The tested samples show the characteristic stretching vibrations absorption peaks of -OH (about 3430 cm^{-1}) and C=C (about 1630 cm^{-1}) caused by the remaining EG, EG_{Fe} and LLDPE. Peaks round 2350 cm^{-1} are stretching vibrations absorption O-C-O. At the same time, the strong stretching vibration absorptions of sulphate are observed in 70LLDPE/30EG and 70LLDPE/30EG_{Fe} at about 1130 cm^{-1}, but there are obvious superimposed peaks round 1050 cm^{-1} in the FTIR of 70LLDPE/15APP/15EG_{Fe}, it is because the absorption peak of S=O and P=O are both appear in the range of 1300-1080 cm^{-1} (Li *et al.*, 1994; Zhao *et al.*, 2004). The specific absorptions of the Fe-O at 721 cm^{-1} and 575 cm^{-1} present both in the residues of 70LLDPE/30EG_{Fe} and 70LLDPE/15APP/15EG_{Fe}, but no peak of NO_3^- is observed. The above results indicate that Fe_2O_3 and APP decomposition products are active in the solid phase of burning materials.

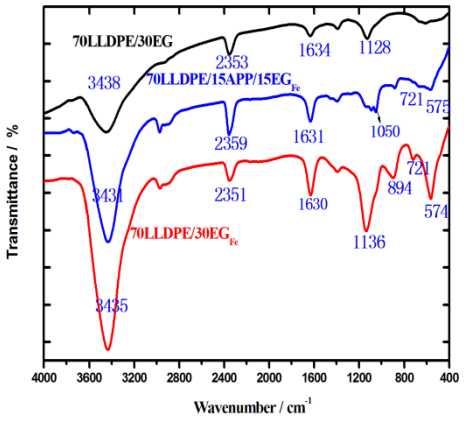

Figure 6: The Combustion Residues FTIR Spectra of the70LLDPE/30EG, 70LLDPE/30EG_{Fe} and 70LLDPE/15APP/15EG_{Fe} Composites

Research Article

Thermal Property of the Flame Retarded LLDPE Composites

Thermal stability of flame retarded LLDPE is related to the addition of additives. TG/DTG analysis under N_2 atmosphere is used to evaluate the thermal degradation properties of 70LLDPE/30EG, 70lLLDPE/30EG_{Fe}, 70LLDPE/30APP, 70LLDPE/15APP/15EG_{Fe} composites and FRs including EG_{Fe}, APP, $Fe(NO_3)_3{\cdot}9H_2O$, mixture of $Fe(NO_3)_3{\cdot}9H_2O$ and APP, the results are showed in Figure 7 and Table 3.

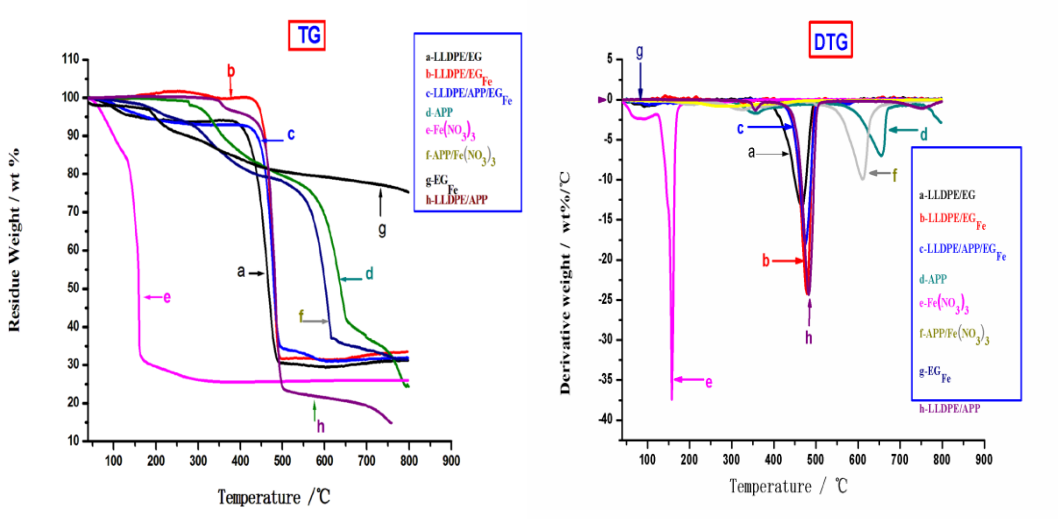

Figure 7: TG/DTG Analysis of 70LLDPE/30EG (a), 70LLDPE/30EG_{Fe} (b), 70LLDPE/15APP/15EG_{Fe} (c), APP (d), $Fe(NO_3)_3{\cdot}9H_2O$ (e), $Fe(NO_3)_3{\cdot}9H_2O$ /APP (f), EG_{Fe} (g) and 70LLDPE/30APP (h)

Table 3: Thermoanalysis Data for Additives and the Flame Retarded LLDPE in N2 Atmosphere c

Specimens	T_{max} °C			R_{max} wt%/°C			Residual Char Yield %	
	I		II		III		R_{exp}	R_{the}
70LLDPE/30EG	468	-13.3	N.D.	N.D.	N.D.	N.D.	31.2	N.D.
70LLDPE/30EG_{Fe}	478	-24.4	N.D.	N.D.	N.D.	N.D.	33.5	30.3
70LLDPE/30APP	355	-1.3	483	-24.3	N.D.	N.D.	12.3	N.D.
70LLDPE/15APP/15EG_{Fe}	475	-18.0	N.D.	N.D.	N.D.	N.D.	31.9	22.9
APP	360	-1.7	655	-7.0	N.D.	N.D.	24.3	N.D.
EG_{Fe}	278	-0.8	N.D.	N.D.	N.D.	N.D.	75.2	N.D.
$Fe(NO_3)_3{\cdot}9H_2O$	158	-37.4	N.D.	N.D.	N.D.	N.D.	25.9	N.D.
$Fe(NO_3)_3{\cdot}9H_2O$ /APP	211	-0.06	323	-1.2	611	-9.9	31.4	24.5

[c] T_{max}: temperature corresponding to the maximum mass loss rate, °C;
R_{max}: the maximum mass loss rate, wt%/°C;
R_{exp}: the residual char yield detected in TG/DTG analysis;
R_{the}: the residual char yield calculated according to the FRs wt % and their R_{exp} value of independent system.

In the mixture of $Fe(NO_3)_3{\cdot}9H_2O$ and APP, the mass ratio of APP to $Fe(NO_3)_3{\cdot}9H_2O$ is 15:2.55 (calculated according to the dosage of APP in 70LLDPE/15APP/15EG_{Fe} and $Fe(NO_3)_3{\cdot}9H_2O$ in EG_{Fe}). The R_{the} of 70LLDPE/30EG_{Fe} is calculated according to the R_{exp} and the dosage of $Fe(NO_3)_3{\cdot}9H_2O$ and 70LLDPE/30EG respectively.

70LLDPE/30EG and 70LLDPE/30EG_{Fe} composites indicate an obvious one-stage degradation profile. When the temperature is below 400 °C, the weight loss is slight and less than 10%. While, about a 60%

value occurs in the range of 400-500 °C, caused by the decomposition of LLDPE and sufficient oxidation of EG and EG_{Fe}. Although, 70LLDPE/30EG_{Fe} holds a higher R_{max} (the maximum decomposition rate) than the 70LLDPE/30EG, it also keeps a higher T_{max} (temperature corresponding to the maximum decomposition rate) and residual char yield (at 800 °C) of 478 °C, 33.5% than the latter of 468 °C and 31.2% respectively. Furthermore, the detected residual char yield (R_{exp}) of 70LLDPE/30EG_{Fe} is higher than the theoretic calculated result (R_{cal}), calculated according to the residue yield of 70LLDPE/30EG, $Fe(NO_3)_3{\cdot}9H_2O$ and their mass ratio in 70LLDPE/30EG_{Fe}. The above results testified the synergistic effect between EG and $Fe(NO_3)_3$, which is caused by the interstitial effect of the Fe_2O_3 produced in $Fe(NO_3)_3$ decomposition reaction (Chen *et al.*, 2007).

The 70LLDPE/30APP composite shows a two-step degradation profile above 300 °C. In the first step of 300-400 °C, a less than 10% weight loss occurs mainly due to the decomposition of APP and the release of NH_3 and H_2O. Then, an accelerating mass loss takes place due to further decomposition of LLDPE and APP at second step of 500-800 °C. The yield of residue at 800 °C is only 12.3%. Temperatures corresponding to the maximum mass loss rate are 355 °C and 483 °C, respectively.

70LLDPE/15APP/15EG_{Fe} composite shows a similar one-step weight loss as the EG and EG_{Fe} flame retarded system, and presents a middle R_{max}, T_{max} and R_{exp}. On the one hand, 70LLDPE/15APP/15EG_{Fe} always holds a higher thermal stability and more residue than the 70LLDPE/30EG. However, it possesses a less residue than 70LLDPE/30EG_{Fe} below 480 °C. Whereas, the residue mass become higher in the range of 480-585 °C, and then lower than that of 70LLDPE/30EG_{Fe} above 585°C. To illuminate the TG results of 70LLDPE/15APP/15EG_{Fe}, TG/DTG tests severally for EG_{Fe}, APP, $Fe(NO_3)_3{\cdot}9H_2O$, mixture of APP and $Fe(NO_3)_3{\cdot}9H_2O$ at a mass ratio of about 15:2.55 (calculated according to the dosage of APP and $Fe(NO_3)_3{\cdot}9H_2O$ in 70LLDPE/15APP/15EG_{Fe}) were carried out.

The mass loss of EG_{Fe} mainly occurs among 200-500 °C, wherein CO_2, H_2O and SO_2 gas released during GIC redox reaction, which leads to the generation of "worm like" expanded graphite. At the same time, the intercalated $Fe(NO_3)_3$ completely decomposes and turns into Fe_2O_3. EG_{Fe} keeps a high residual char yield of 75.2% at 800 °C.

APP shows a two-step degradation profile above 300 °C. In the first step of 300-500 °C, the evolution products are mainly NH_3, H_2O gases and polyphosphoric acids (Zhou *et al.*, 2013), which cause a mass decrease of about 20% with a slow rate. Then, an accelerating mass loss takes place due to the release of the volatile P_2O_5 at second step of 500-800 °C, and then reserves a residue yield of 24.3% at 800 °C.

$Fe(NO_3)_3{\cdot}9H_2O$ shows poor thermal stability below 300 °C, and the decomposition reaction will finish when the temperature is above 300 °C. The residue yield is detected as 25.9%.

As for the mixture of $Fe(NO_3)_3{\cdot}9H_2O$ and APP, it presents a three-step degradation profile. The first stage is caused by the weight loss of $Fe(NO_3)_3{\cdot}9H_2O$ and with a $T_{max,I}$ of 211 °C. The second and third stages are mainly caused by the decomposition and weight loss of APP with a $T_{max,II}$ of 323 °C and $T_{max,III}$ of 611 °C, which shift to the lower temperature than the independent APP of 360 °C and 655 °C. But once the decomposition finished, this mixture will keep a higher thermal stability, reflected by the improved residue yield of 31.6% at 800 °C, which is higher than the R_{the} of 24.5% calculated according to R_{exp} of APP, $Fe(NO_3)_3{\cdot}9H_2O$ and their mass ratio. The lower $T_{max,II}$, $T_{max,III}$ and high final residual yield should be caused by the reaction between Fe_2O_3 and polyphosphoric acids. It has been testified that Fe_2O_3 can accelerate the decomposition reaction of APP, and then form stable polyphosphate (Zhou *et al.*, 2013). These results can provide evidence for the 70LLDPE/15APP/15EG_{Fe} holding more residues in the range of 480-585 °C due to the formation of polyphosphate, and then it's lower than that of 70LLDPE/30EG_{Fe} due to the addition of EG_{Fe} with high R_{exp} and wt %.

Possible Flame Retardant Mechanism

Combining the LOI and vertical combustion UL 94 results and associating with the residue macrostructures, micromorphology and FTIR, TG/DTG characteristics of the flame retarded LLDPE composites, it can be described as Figure 8. When contacting with flame source, EG_{Fe} will instantly expand and turn into swollen multi cellular "graphite worms" covering on the matrix surface, which is in favor of slowing down the heat and mass transfer and interrupting polymer degradation. Moreover,

expansion of EG_{Fe} and decomposition of $Fe(NO_3)_3$ will consume an enormous amount of heat, which is helpful to decrease the combustion temperature and rate. Furthermore, oxidation reaction between graphite and H_2SO_4 releases CO_2, H_2O and SO_2, which can reduce combustible gas concentration and then enhance the char formation. The intervention of Fe_2O_3 and APP are active in the solid phase of burning materials. When heated, $Fe(NO_3)_3$ will produce Fe_2O_3, which will then accelerate APP release NH_3, H_2O and produce polyphosphoric acid at relative low temperature. The produced polyphosphoric acid can further react with Fe_2O_3 and lead to the formation of stable polyphosphate. It is the interstitial filling of Fe_2O_3 and polyphosphate, together with the conglutination between the loose "graphite worms" by polyphosphoric acid that further enhance the continuous and compact of char layers, suppress the "popcorn effect" and avoid the direct contact between substrate and flame. All these make 70LLDPE/15APP/15EG_{Fe} composite show better flame retardation, and there is not only physical synergy, but also chemical reaction between the additives.

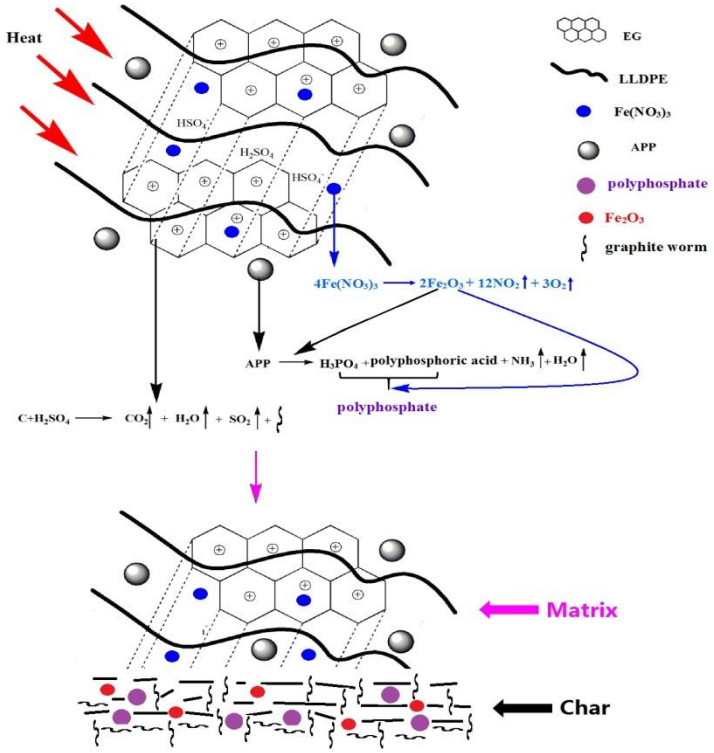

Figure 8: The Flame Retardant Mechanism of LLDPE/APP/EG_{Fe} System

Conclusion

Ferric nitrate modified EG_{Fe} was successfully prepared with H_2SO_4 and $Fe(NO_3)_3 \cdot 9H_2O$ as intercalator and assistant intercalator in graphite oxidation and intercalation reaction. Compared with the normal EG, EG_{Fe} possessed a better dilatability, flame retardancy and environment-friendly property. SEM, EDS, FTIR and XRD confirmed the oxidation and intercalation reaction between the reactants. EG_{Fe} exhibited better LOI and UL-94 level for LLDPE than the normal EG. Moreover, the combination of EG_{Fe} with APP showed more excellent flame retardancy. The generated Fe_2O_3 could not only impel APP to release NH_3, H_2O, produce polyphosphoric acid at relative low temperature, but also form stable polyphosphate and then improve LLDPE composites thermal stability at high temperature due to the continuous and compact char layers. The interstitial filling of Fe_2O_3 and polyphosphate together with the conglutination between the loose "graphite worms" by polyphosphoric acid suppressed the "popcorn effect" and avoided the direct contact between substrate and flame at some extent. The physical synergy and chemical interaction between the used FRs made 70LLDPE/15APP/15EG_{Fe} composite show excellent flame

retardation.

ACKNOWLEDGEMENT
The authors would like to thank Natural Science Foundation of Hebei Province (CN) (No. B2015201028) and Seedling Project of College of Chemistry and Environmental Science (Hebei University) for financial support.

REFERENCES

Ebert LB (1976). Intercalation compounds of graphite. *Annual Review of Materials Science* **6** 181-211.

Camino G, Martinasso G and Costa L (1990). Thermal degradation of pentaerythritol diphosphate, model compound for fire retardant intumescent systems: Part I-Overall thermal degradation. *Polymer Degradation and Stability* **27**(3) 285-96.

Chen XL, Wu H, Luo Z, Yang B, Guo SY and Yu J (2007). Synergistic effects of expandable graphite with magnesium hydroxide on the flame retardancy and thermal properties of polypropylene. *Polymer Engineering & Science* **47**(11) 1756-60.

Duquesne S, Michel LB, Bourbigot S, Delobel R, Vezin H, Camino G, Eling B, Lindsay C, and Roels T (2003). Expandabie graphite: a fire retardant additive for polyurethane coatings. *Fire and Materials* **27**(3) 103-17.

Gaan S, Sun G, Hutches K and Engelhard MH (2008). Effect of nitrogen additives on flame retardant action of tributyl phosphate: Phosphorus-nitrogen synergism. *Polymer Degradation and Stability* **93**(1) 99-108.

Gao HL, Hu S, Han HC and Zhang J (2011). Effect of different metallic hydroxides on flame-retardant properties of low density polyethylene/melamine polyphosphate/starch composites. *Journal of Applied Polymer Science* **122**(5) 3263-9.

Ge LL, Duan HJ, Zhang XG, Chen C, Tang JH and Li ZMJ (2012). Synergistic effect of ammonium polyphosphate and expandable graphite on flame-retardant properties of acrylonitrile-butadiene-styrene. *Journal of Applied Polymer Science* **126**(4) 1337-43.

Han ZD, Zhang DW, Dong LM and Zhang XY (2007). Preparation of expandable graphite intercalated by ammonium phosphate and ammonium polyphosphate. *Chinese Journal of Inorganic Chemistry* **23**(2) 286-90.

Horacek H and Grabner R (1996). Advantages of flame retardants based on nitrogen compounds. *Polymer Degradation and Stability* **54**(2) 205-15.

Hu XM and Wang DM (2013). Enhanced fire behavior of rigid polyurethane foam by intumescent flame retardants. *Journal of Applied Polymer Science* **129**(1) 238-46.

Kemmlein S, Hahn O and Jann O (2003). Emissions of organophosphate and brominated flame retardants from selected consumer products and building materials. *Atmospheric Environment* **37**(3) 5485-93.

Lai XJ, Yin CY, Li HQ and Zeng XR (2015). Synergistic effect between silicone-containing macromolecular charring agent and ammonium polyphosphate in flame retardant polypropylene. *Journal of Applied Polymer Science* **132**(10) DOI: 10.1002/APP.41580.

Li H, Zhang JW and Wang XH (1994). Identification of unknown components by Fourier infrared spectrometer. *Chinese Journal Front Health Quarantine* **17**(5) 98-100.

Liu JC, Zhang YB, Yu ZL, Yang WY, Luo J, Pan BL and Lu C (2016). Enhancement of organoclay on thermal and flame retardant properties of polystyrene/magnesium hydroxide composite. *Polymer Composites* **37**(3) 746-55.

Lu C, Cao QQ, Hu XN, Liu CY, Huang XH and Zhang YQ (2014). Influence of morphology and

ammonium polyphosphate dispersion on the flame retardancy of polystyrene/nylon-6 blends. *Fire and Materials* **38**(8) 765-76.

Menachem L (2001). Synergism and catalysis in flame retardancy of polymers. *Polymers for Advanced Technologies* **12**(3-4) 215-22.

Meng X Y, Ye L, Zhang X G, Tang PM and Tang JH (2009). Effects of expandable graphite and ammonium polyphosphate on the flame-retardant and mechanical properties of rigid polyurethane foams. *Journal of Applied Polymer Science* **114**(2) 853-63.

Modesti M, Lorenzetti A, Simioni F and Camino G (2002). Expandable graphite as an intumescent flame retardant in polyisocyanurate polyurethane foams. *Polymer Degradation and Stability* **77**(2) 195-202.

Nie SB, Hu Y, Song L, He QL, Yang DD and Chen H (2008). Synergistic effect between a 84 (CFA) and microencapsulated ammonium polyphosphate on the thermal and flame retardant properties of polypropylene. *Polymers for Advanced Technologies* **19**(8) 1077-83.

Pang XY, Duan MW, Zhai ZX and Tian Y (2015). An intumescent flame retardant-expandable graphite: Preparation, characteristics and flame retardance for polyethylene. *Kuwait Journal of Science* **42**(1) 133-49.

Seefeldt H, Braun U and Wagner MH (2012). Residue stabilization in the fire retardancy of wood-plastic composites: combination of ammonium polyphosphate, expandable graphite, and red phosphorus. *Macromolecular Chemistry and Physics* **213**(22) 2370-77.

Shi L, Li ZM, Xie BH, Wang JH, Tian CR and Yang MB (2006). Flame retardancy of different-sized expandable graphite particles for high-density rigid polyurethane foams. *Polymer International* **55**(8) 862-71.

Shioyam H and Fujii R (1987). Electrochemical reactions of stage 1 sulfuric acid-Graphite intercalation compound. *Carbon* **25**(6) 771-4.

Shornikova ON, Dunaev AV, Maksimova NV and Avdeev VV (2006). Synthesis and properties of ternary GIC with iron or copper chlorides. *Journal of Physics and Chemistry of Solids* **67**(5–6) 1193-7.

Song KM, Li GS, Feng YL and Yan QY (1996). Preparation of low-sulfur expansible graphite by using mixing acid. *Chinese Journal of Inorganic Materials* **11**(4) 749-52.

Sun ZD, Ma YH, Xu Y, Chen XL, Chen M, Yu J, Hu SC and Zhang ZB (2014). Effect of the particle size of expandable graphite on the thermal stability, flammability, and mechanical properties of high-density polyethylene/ethylene vinyl-acetate/expandable graphite composites. *Polymer Engineering & Science* **54**(5) 1162-69.

Tang MQ, Qi F, Chen M, Sun ZD and Xu Y (2016). Synergistic effects of ammonium polyphosphate and red phosphorus with expandable graphite on flammability and thermal properties of HDPE/EVA blends. *Polymers for Advanced Technologies* **27**(1) 52-60.

Willeams DH and Fleing I (2001). *Spectral Method in Organic Chemistry*, translated by Wang JB and Shi WF, (Beijing University Press, Beijing, China).

Xie RC and Qu BJ (2001). Expandable graphite systems for halogen-free flame-retarding of polyolefins. II. Structures of intumescent char and flame-retardant mechanism. *Journal of Applied Polymer Science* **80**(8) 1190-7.

Xu DM, Ding F, Hao JW and Du JX (2013). Preparation of modified expandable graphite and its flame retardant application in rigid polyurethane foam. *Chemical Journal of Chinese University* **34**(11) 2674-80.

Zhang J, Horrocks AR and Hall ME (2010). The flammability of polyacrylonitrile and its copolymers IV. The flame retardant mechanism of ammonium polyphosphate. *Fire and Materials* **18**(5) 307-12.

Zhang Y, Chen XL and Fang ZP (2013). Synergistic effects of expandable graphite and ammonium polyphosphate with a new carbon source derived from biomass in flame retardant ABS. *Journal of*

Applied Polymer Science **128**(4) 2424-32.

Zhao C, Gu XJ, Zhong SH and Xiao XF (2004). Study on the reaction behaviors of forming propylene oxide from 1,2-dichloropane on Fe-Al-P-O catalyst. *Journal of Chemical Engineering of Chinese University* **18**(4) 510-4.

Zheng ZH, Sun HM, Li WJ, Zhong SL, Yan JT, Cui XJ and Wang HY (2013). Co-microencapsulation of ammonium polyphosphate and aluminum hydroxide in halogen-free and intumescent flame retarding polypropylene. *Polymer Composites* **35**(4) 715-29.

Zhou Y, Hao JW, Liu GS and Du JX (2013). Influencing mechanism of transition metal oxide on thermal decomposition of ammonium polyphosphate. *Chinese Journal of Inorganic Chemistry* **29**(6) 1115-22.